
Article:
Huang, Z. orcid.org/0000-0002-6529-8691, Brennen, G.K. orcid.org/0000-0002-6019-966X and Ouyang, Y. orcid.org/0000-0003-1115-0074 (2022) Imaging stars with quantum error correction. Physical Review Letters, 129 (21). 210502. ISSN 0031-9007

https://doi.org/10.1103/physrevlett.129.210502

Imaging stars with quantum error correction

Zixin Huang,[1,*] Gavin K. Brennen,[1,†] and Yingkai Ouyang[2,3,‡]

[1] *Centre for Engineered Quantum Systems, School of Mathematical and Physical Sciences, Macquarie University, NSW 2109, Australia*
[2] *Department of Electrical and Computer Engineering, National University of Singapore, Singapore*
[3] *Centre of Quantum Technologies, National University of Singapore, Singapore*

(Dated: April 14, 2022)

The development of high-resolution, large-baseline optical interferometers would revolutionize astronomical imaging. However, classical techniques are hindered by physical limitations including loss, noise, and the fact that the received light is generally quantum in nature. We show how to overcome these issues using quantum communication techniques. We present a general framework for using quantum error correction codes for protecting and imaging starlight received at distant telescope sites. In our scheme, the quantum state of light is coherently captured into a non-radiative atomic state via Stimulated Raman Adiabatic Passage, which is then imprinted into a quantum error correction code. The code protects the signal during subsequent potentially noisy operations necessary to extract the image parameters. We show that even a small quantum error correction code can offer significant protection against noise. For large codes, we find noise thresholds below which the information can be preserved. Our scheme represents an application for near-term quantum devices that can increase imaging resolution beyond what is feasible using classical techniques.

I. INTRODUCTION

The performance of an imaging system is limited by diffraction: the resolution is proportional to its aperture and inversely proportional to the wavelength λ. Together these place a fundamental limit on how well one can image the objects of interest. Typical techniques employed to enable quantum sensing and quantum imaging to surpass classical limits utilise entanglement [1, 2], source engineering (fluorescence microscopy [3]), or squeezing [4] to suppress intensity fluctuations. These techniques require manipulating the objects or illuminating them with light that has special properties. However, often it is the case, such as for astronomy, that we have neither direct access to, nor the ability to illuminate the objects of interest. Rather all we can do is analyse the light that reaches us.

To maximise imaging resolution, the experimenter aims to use large apertures and small wavelengths. High-resolution imaging requires not only intensity measurements, but also the phase relationship in different parts of the imaging system to be well-established. Current large-baseline telescope arrays [5] operate in the microwave and radio-frequency domains, because we can measure the phase as well as the amplitude of the received signal directly. By moving into optical frequencies, we can increase the resolution by a factor of $\lambda_{\text{optical}}/\lambda_{\text{microwave}}$, a three to five orders of magnitude improvement. An optical interferometer the size of the planet's diameter would be powerful enough to image small planets around nearby stars [6], details of solar systems, kinematics of stellar surfaces [7], and potentially details around black-hole event horizons – none of which currently planned projects can resolve.

However, this task is extremely challenging, because even the fastest electronics cannot directly measure the oscillations of electric fields at optical frequencies. Several challenges hinder the progress in building large-baseline optical interferometers, one of which is the presence of noise and transmission loss that ultimately limits the distance between telescope sites. To avoid transmission losses, in the most direct approach [8], we could store the signal into atomic states and perform operations to extract the information; however, such states are sensitive to optical decay and other decoherence. One way to combat noise in physical systems is to employ quantum error correction (QEC). QEC has been predominantly studied for in the context of quantum computation [9] and specialised sensing protocols [10–19].

In this paper, we produce a general framework for using QEC codes to protect the information in the received light. This is the first time that QEC has been applied to a quantum parameter estimation task where the probe state need not be prepared by the experimenter. We eliminate optical decay in quantum memories by coupling light into non-radiative atomic qubit states via the well-developed process known as STImulated Raman Adiabatic Passage (STIRAP) [20]. Then, the state in the quantum memories is imprinted onto a QEC code, thus protecting the signal from subsequent, potentially noisy operations. In addition, when the signal arrives, there are potential multi-photon events, which our scheme can accommodate. Two general proof-of-principle results [8, 21] have investigated the potential for entanglement-aided imaging, when the quantum memories and subsequent quantum operations are ideal. Here we take into account for noise sources such as optical decay and propose a robust encoding of the signal into quantum memories.

* zixin.huang@mq.edu.au
† gavin.brennen@mq.edu.au
‡ oyingkai@gmail.com

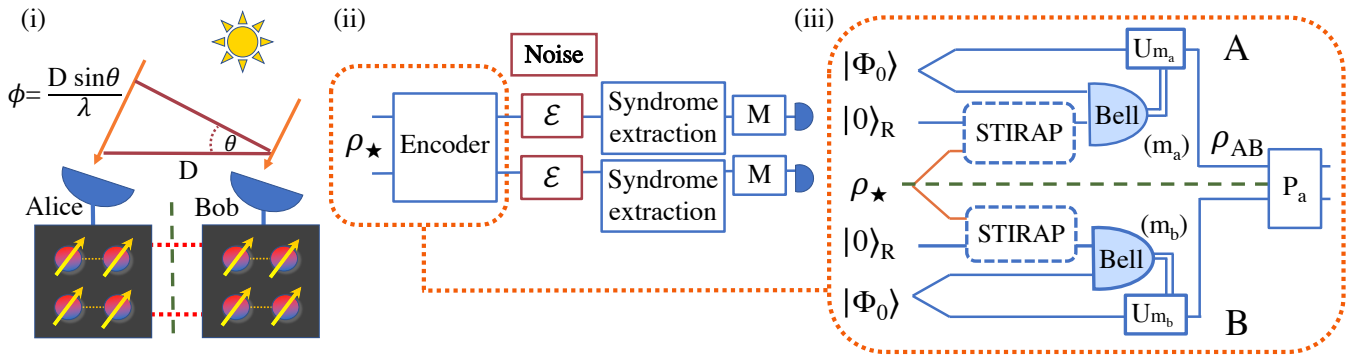

FIG. 1. **Overview of our protocol.** (i) Light at wavelength λ from astronomical sources is collected at two sites, Alice and Bob, separated by a distance D with each holding a quantum memory and sharing one or more Bell pairs. (ii) A general framework for the process encoding, error correction, and measurement of the signal. The starlight $\rho_\star$ is input into an encoder, which outputs a logical state of a quantum code. The memory qubits and subsequent operations are potentially noisy as modelled by local channels $\mathcal{E}$. Any correctible error is detected by syndrome measurements and the final step is a local Clifford measurement M, that depends on the error syndromes, and that extracts the parameters of interest from the state. (iii) A more detailed schematic that shows the operations to encode the starlight into a protected logical state. The green dashed line denotes the spatial separation between Alice and Bob. U_m are Pauli corrections depending on the outcome of local Bell measurements. The operation P_a is a parity measurement to project out the vacuum component of light (and possible multiphoton contributions) and is the only part of the protocol that uses non-local resources.

Any imaging task can be translated into a parameter estimation task, where the quantity of interest is the quantum Fisher information (QFI). We show that even a small QEC code can offer significant protection against noise which degrades resolution. For small QEC codes, one can calculate the QFI directly. However, the computational complexity of the calculation grows exponentially with the number of qubits. For large QEC codes, the QFI can be preserved, provided that the noise is below a certain threshold. Our bounds on the QFI in this case are both analytical and asymptotically tight.

The structure of the paper follows. In Sec II we give an overview of the entire protocol; in Sec. III, we describe our model of the astronomical signal and briefly review the quantum Fisher information formalism. In Sec. IV, we describe STIRAP and show how to find the pulse shape necessary to transfer the photon into the atomic qubit with near unit fidelity, followed by Sec. V, where we explain the encoding process. In Sec. VI, we show quantitatively how quantum error correction can protect the QFI. In the Supplemental Information, we show how the unprotected state performs under various noise models, and describe how to accommodate for higher photon contributions.

II. THE PROTOCOL

We show an overview of our protocol in Fig. 1. We consider a two-site scenario, denoted Alice and Bob, where each holds a telescope station and they are separated by a long distance. The layer of quantum technology is schematically shown in panel (i), where light from astronomical sources is collected by Alice and Bob: they share pre-distributed entanglement, and each of the two sites contains quantum memories into which the light is captured. This becomes part of the encoder operation depicted in panel (ii), which shows a general framework for imprinting the signal into a quantum error correction code. Here Alice and Bob each prepares (locally) their set of qubits into some QEC code. The received state $\rho_\star$ is imprinted onto the code via an encoder, resulting in the logical state ρ_{AB} shared between Alice and Bob. The state is thus protected from subsequent noisy operations. Panel (iii) shows the circuit of the encoder, which is described in detail in Sec. V. The green dashed line represents the spatial separation between Alice and Bob. The pre-distributed entanglement is used to project onto the single photon subspace of $\rho_\star$. One Bell-pair suffices to filter out the vacuum, and two will filter out the vacuum and the much smaller component of two photon states.

In the "encoder" stage, we need to capture the signal into the quantum memories, which involves a light-matter interaction Hamiltonian. In the naive approach, we could use two-level atoms with ground and excited state encoding, $|g\rangle, |e\rangle$, where the energy difference corresponds to the energy of the photon. If we were to place such an ensemble of excited atoms in a cavity, the atoms will undergo optical decay that can introduce errors or take the state outside the codespace altogether. To circumvent this, we use a scheme known as STImulated Raman Adiabatic Passage (STIRAP) which allows us to coherently couple the incoming light into a non-radiative state of an atom. Unlike the naive approach, we do not need to match the frequency of the signal with the atomic transition, giving us more bandwidth and flexibility. The state is then imprinted onto a QEC code via a Bell measurement. Details follow.

III. THE MODEL

We model the incoming signal as a weak thermal state of light [22] that has been multiplexed into frequency bands narrow enough for interferometry. For such an n-mode Gaussian state, for a particular band, given density matrix ρ and the creation/annihilation operators $P = (a_1, a_1^\dagger, ..., a_n, a_n^\dagger)$, its properties are completely specified by the first and second moments

$$\mu_k = \mathrm{Tr}[P_k \rho], \qquad \Sigma_{k,l} = \frac{1}{2}\mathrm{Tr}[\{P_k - \mu_k, P_l - \mu_l\}\rho] \quad (1)$$

where $\{X, Y\} = XY + YX$ denotes the anticommutator. In basis $\{a, a^\dagger, b, b^\dagger\}$, where a (b) is the annihilation operator of the mode held by Alice (Bob), we have the first moments equal to 0, and the covariance matrix

$$\Sigma = \begin{pmatrix} 0 & \frac{\epsilon}{2}+\frac{1}{2} & 0 & \frac{1}{2}\gamma\epsilon e^{i\phi} \\ \frac{\epsilon}{2}+\frac{1}{2} & 0 & \frac{1}{2}\gamma\epsilon e^{-i\phi} & 0 \\ 0 & \frac{1}{2}\gamma\epsilon e^{-i\phi} & 0 & \frac{\epsilon}{2}+\frac{1}{2} \\ \frac{1}{2}\gamma\epsilon e^{i\phi} & 0 & \frac{\epsilon}{2}+\frac{1}{2} & 0 \end{pmatrix}, \quad (2)$$

here $\epsilon/2$ is the mean photon number of both modes.

The parameters of interest are ϕ and γ, where $\phi \in [0, 2\pi)$ is related to the location of the sources, and $\gamma \in [0, 1]$ is proportional to the Fourier transform of the intensity distribution (shape of the objects) via the van Cittert-Zernike theorem [22]. Optimally estimating ϕ and γ provides complete information of the source distribution by using two modes [23]. In this paper, we consider the optimal estimation of two-mode states for clarity; this easily extends to multi-mode, broadband operation by incorporating the time and frequency-multiplexed encoding in Refs. [8, 24].

The ultimate precision in the estimation is given by the quantum Cramér-Rao bound [1, 2, 25, 26]. For the estimation of the parameter φ encoded onto a quantum state ρ_φ, this is a lower bound on the variance $(\Delta\hat{\varphi})^2 = \langle\hat{\varphi}^2\rangle - \langle\hat{\varphi}\rangle^2$ of any unbiased estimator $\hat{\varphi}$. For unbiased estimators, the quantum Cramer-Rao bound establishes that

$$(\Delta\hat{\varphi})^2 \geqslant \frac{1}{N}\frac{1}{J(\rho_\varphi)}, \quad (3)$$

where N is the number of probe systems used, and J is the quantum Fisher information (QFI) associated with the global state ρ_λ of the probes. The latter is defined as

$$J(\rho_\varphi) = \mathrm{Tr}\left(L_\varphi^2 \rho_\varphi\right), \quad (4)$$

where L_φ is the Symmetric Logarithmic Derivative (SLD) associated with the parameter φ [27]. Consider a set of basis vectors $|e_1\rangle$, $|e_2\rangle$, ... in which ρ_φ is diagonal:

$$\rho_\varphi = \sum_n p_n |e_n\rangle\langle e_n|. \quad (5)$$

The SLD is then given by

$$L_\varphi = 2 \sum_{n,m:p_n+p_m\neq 0} \frac{\langle e_m|\partial_\varphi\rho|e_n\rangle}{p_n + p_m} |e_m\rangle\langle e_n|, \quad (6)$$

with $\partial_\varphi\rho = \partial\rho_\varphi/\partial\varphi$. The quantum Cramer-Rao bound is asymptotically saturated in the limit that $N \to \infty$ [28].

If multiple parameters are to be estimated, a necessary and sufficient condition for their joint optimal estimation is [29]

$$\mathrm{Tr}(\rho_{\boldsymbol{\varphi}}[L_{\varphi_i}, L_{\varphi_j}] = 0). \quad (7)$$

The condition in Eq. (7) is not satisfied for ϕ and γ, which means they will need to be separately estimated.

First, consider the case where most of the time, at most a single photon arrives on the two sites, i.e. $\epsilon \ll 1$. We can describe the optical state by the density matrix

$$\rho_\star = (1-\epsilon)|\mathrm{vac,vac}\rangle\langle\mathrm{vac,vac}|_{AB} + \epsilon\left(\frac{1+\gamma}{2}\right)|\psi_+^\phi\rangle\langle\psi_+^\phi| + \epsilon\left(\frac{1-\gamma}{2}\right)|\psi_-^\phi\rangle\langle\psi_-^\phi| + O(\epsilon^2) \quad (8)$$

where $|\psi_\pm^\phi\rangle = (|1_p\rangle_A|\mathrm{vac}\rangle_B \pm e^{i\phi}|\mathrm{vac}\rangle_A|1_p\rangle_B)/\sqrt{2}$. Here the subscript p denotes a photon Fock state of the corresponding photon number. To coherently couple this state into the quantum memories, we use the STIRAP interaction.

IV. STIMULATED RAMAN ADIABATIC PASSAGE

STIRAP is inherently robust to parameter errors and resilient to certain types of noise, and has emerged as a popular tool in quantum information. Notably, it is immune to loss through spontaneous emission (amplitude damping), and robust against small variations of experimental conditions, such as laser intensity, pulse timing, and pulse shape [20].

We depict our set-up in Fig. 2: (a) inside a cavity, we use three different sets of systems. We denote the blue array as the register. The blue array is initialised in a codespace of a QEC code encoding a single logical qubit, spanned by its logical codewords $|0_L\rangle$ and $|1_L\rangle$. We also need ancilla qubit 1 (green), and ancilla atom 2 (red). Note the three types of matter qubits could consist of different electronic sublevels of the same species of atom if desired.

In panel (b) we describe the energy levels of ancilla atom 2. This atom has three energy levels: the excited state $|e\rangle$, and two ground state levels, $|0\rangle_R$ and $|1\rangle_R$ that for convenience we have assumed degenerate, though this is not essential. The energy difference between $|0\rangle_R$ and $|e\rangle$ is ω_0. Ancilla atom 2 is optically trapped. The cavity coupling between $|0\rangle_R$ and $|e\rangle$ is denoted g, which is a fixed parameter that depends on the properties of the

atom and the cavity; the time-dependent Rabi frequency on the transition $|1\rangle_R$ to $|e\rangle$ is denoted $\Omega(t)$. The parameter $\Omega(t)$ is tunable via changing the intensity of another laser, which has frequency ω_L, and has detuning Δ from ω_0.

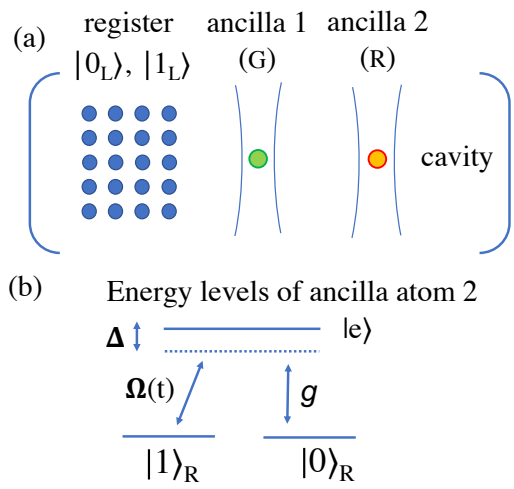

FIG. 2. **Cavity-assisted coherent single-photon transfer.** (a) A system of qubits has logical states $|0_L\rangle, |1_L\rangle$; ancillary qubit 1 is initially prepared into a Bell state with the register, $1/\sqrt{2}(|0_L 0_G\rangle + |1_L 1_G\rangle)$; ancilla 2 is used in the STIRAP interaction to interact with the star photon. (b) Energy levels the ancilla atom 2 used for the STIRAP interaction.

Defining n to be the number of photons in the cavity, the STIRAP Hamiltonian is

$$\begin{aligned} H_{\text{stirap}}(t) = \omega_0 |e\rangle\langle e| + \omega_c a^\dagger a + \\ \Omega(t) e^{-i\omega_L t} |e\rangle\langle 1| + \Omega(t)^* e^{i\omega_L t} |1\rangle\langle e| + \\ g a |0\rangle\langle e| + g^* a^\dagger |e\rangle\langle 0| . \end{aligned} \tag{9}$$

In the rotating wave approximation, in the basis $\{|1_R, n-1\rangle, |e, n-1\rangle, |0_R, n\rangle\}$, the interaction Hamiltonian can be written as a direct sum,

$$H_I(t) = \sum_n H^{(n)}(t), \quad H^{(n)}(t) = \begin{pmatrix} 0 & \Omega(t)^* & 0 \\ \Omega(t) & -\Delta & g\sqrt{n} \\ 0 & g^*\sqrt{n} & 0 \end{pmatrix}. \tag{10}$$

Here $\Delta = \omega_L - \omega_0$, which is the energy difference between the laser and the transition energy and itself can be a function of time. One of the eigenstates of $H^{(n)}(t)$ has a zero eigenvalue, $H^{(n)}(t)|\psi_0(t)\rangle = 0$, where

$$\begin{aligned} |\psi_0(t)\rangle &= c\left(-r(t)|1\rangle_R |n-1\rangle + |0\rangle_R |n\rangle\right), \\ r(t) &= \frac{g\sqrt{n}}{\Omega(t)} \end{aligned} \tag{11}$$

and c is a normalisation factor.

Before the interaction, the initial state is $|0\rangle_R$, and this will be the eigenstate if $\Omega(t=0) \gg g$. Then, if we adiabatically tune down $\Omega(t)$ such that at the end of the interaction, $t = T$, if $\Omega(T) \ll g$, then $|\psi(T)\rangle \approx |1\rangle_R$. That is, we have made a controlled spin population transfer from $|0\rangle_R$ to $|1\rangle_R$ depending on the presence of the photon. If the photon is absent, $|0\rangle_R |\text{vac}\rangle$ stays as $|0\rangle_R |\text{vac}\rangle$. The joint state of the atom-photon evolves as $\rho(T) = U_I(T)\rho(0)U_I^\dagger(T)$, $U_I(T) = \mathcal{T}\left\{\int_0^T \exp(-iH_I t)dt\right\}$, where $\mathcal{T}\{\cdot\}$ is the time-ordering operator. Since we stay in the 0 eigenvalue of $H(t)$ for all time there is no dynamical phase accumulated. This is what makes STIRAP robust against timing errors.

In Fig. 3, for $n = 1$, we show that the population transfer between the atomic states $|0\rangle_R$ and $|1\rangle_R$ can be completed without populating the excited state $|e\rangle$, thus avoiding spontaneous emission. We have fixed the parameter $g = 1$, and $\Omega(t)$ is numerically optimised to maximise the transfer from $|0\rangle_R$ to $|1\rangle_R$. The pulse is divided into three intervals for $\Omega(t)$: during the first interval, $\Omega(t)$ is linear, in the second interval, it is a hyperbolic tangent function, and finally, a short linear taper to ensure $\Omega(T) = 0$. Note that during the STIRAP pulse there is a possibility of dephasing on the red ancilla qubits. However, this dephasing can be mitigated by judicious choice of ground states. For example, in an alkali atom with hyperfine structure and half integer nuclear spin ($I > 1$) one could choose the states $|0\rangle_R = |F_\uparrow, M_F = 1\rangle$, $|1\rangle_R = |F_\downarrow, M_F = -1\rangle$, and $|e\rangle = |F', M_F = 0\rangle$. Because the Landé g-factors are equal and opposite for the two ground state hyperfine manifolds, the shift due to extraneous magnetic fields will be zero to first order. Additionally, with this choice of levels, a time dependent detuning $\Delta(t)$ to satisfy adiabaticity can be realized by turning on a time dependent magnetic field along the quantization axis of the atom [30].

V. THE ENCODER

Suppose we now prepare the register and the green ancilla (here the subscript G denotes green) in the Bell state

$$|\Phi_0\rangle = \frac{1}{\sqrt{2}}(|0_L\rangle |0_G\rangle + |1_L\rangle |1_G\rangle). \tag{12}$$

Now, the red ancilla is initially prepared in state $|0\rangle_R$, so our set-up is in state

$$|\Psi_0\rangle = |\Phi_0\rangle \otimes |0\rangle_R . \tag{13}$$

Suppose Alice and Bob each has a copy of $|\Psi_0\rangle$, and they perform STIRAP individually (Fig. 1 panel (iii)). They share the single photon from the star

$$\frac{1}{\sqrt{2}}(|1_p\rangle_A |\text{vac}\rangle_B \pm e^{i\phi} |\text{vac}\rangle_A |1_p\rangle_B). \tag{14}$$

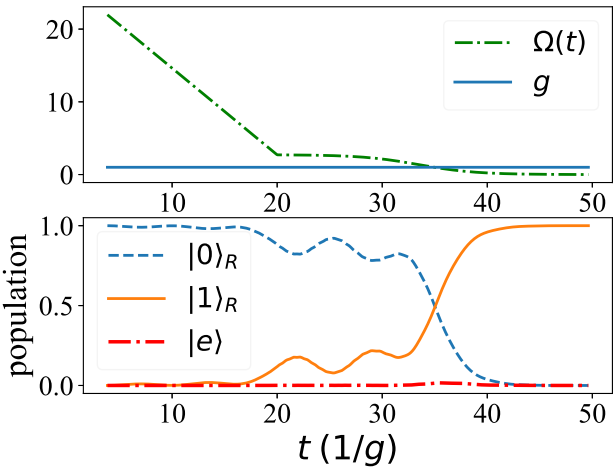

FIG. 3. **Population transfer for of a three-state adiabatic passage**. Top: the interaction strengths of g and Ω as a function of time t in units of $1/g$. Bottom: occupancy of in $|e\rangle, |0\rangle_R$ and $|1\rangle_R$ in ancillary atom 2 (r). The detuning parameter is set to $\Delta(t) = g^2 + \Omega^2(t)$ to satisfy the adiabatic condition [31]. Note that the excited state $|e\rangle$ is not populated.

In the presence of the photon, the STIRAP interaction transforms $|0\rangle_R \to |1\rangle_R$, and the phase relationship in the photon is preserved. This means that the state of the red ancillae (on Alice and Bob's sites) is now

$$\frac{1}{\sqrt{2}}\left(|1_R, 0_R\rangle_{AB} \pm e^{i\phi}\,|0_R, 1_R\rangle_{AB}\right). \tag{15}$$

Performing a Bell measurement on the red and green ancillae teleports the state onto the registers. After the Pauli operator correction dependent on the measurement outcome, the state of the registers between Alice and Bob becomes an entangled state, and the entanglement arises entirely from the starlight photon.

Since the initial starlight state is mixed, after the encoding, the density matrix shared between Alice and Bob is

$$\begin{aligned}\rho_{AB} \approx &(1-\epsilon)\,|0_L0_L\rangle\langle 0_L0_L|_{A_1B_1} + \\ &\epsilon\left(\frac{1+\gamma}{2}\right)|\psi^{\phi}_{+,L}\rangle\langle\psi^{\phi}_{+,L}| + \epsilon\left(\frac{1-\gamma}{2}\right)|\psi^{\phi}_{-,L}\rangle\langle\psi^{\phi}_{-,L}| \\ &+ O(\epsilon^2),\end{aligned} \tag{16}$$

where $|\psi^{\phi}_{\pm,L}\rangle = (|0_L, 1_L\rangle \pm e^{i\phi}\,|1_L, 0_L\rangle)/\sqrt{2}$.

The states $|\psi^{\phi}_{\pm,L}\rangle$ are orthogonal to $|0_L0_L\rangle$ and $|1_L1_L\rangle$, and therefore can be distinguished via a parity measurement [8]. We can introduce additional pre-shared logical Bell pairs $|\Phi^{\pm}\rangle = (|0_L, 0_L\rangle \pm |1_L, 1_L\rangle)/\sqrt{2}$, which can be prepared by injecting a two-qubit Bell pair into Alice and Bob's QEC code by state injection [32]. The quality of the logical Bell pairs can be guaranteed by using distillation protocols [33]. Introducing additional pre-shared logical Bell pairs $|\Phi^{\pm}\rangle = (|0_L, 0_L\rangle \pm |1_L, 1_L\rangle)/\sqrt{2}$, logical CZ gates between the memory qubits in ρ_{AB} and $|\Phi^+\rangle$ can project out the vacuum:

$$\begin{aligned}\rho_{AB}\otimes|\Phi^+\rangle \overset{2\times\mathrm{CZ}}{\to} &|0_L, 0_L\rangle\langle 0_L, 0_L|_{AB}\otimes|\Phi^+\rangle\langle\Phi^+| + \\ &\epsilon\left(\frac{1+\gamma}{2}\right)|\psi^{\phi}_{+,L}\rangle\langle\psi^{\phi}_{+,L}|\otimes|\Phi^-\rangle\langle\Phi^-| + \\ &\epsilon\left(\frac{1-\gamma}{2}\right)|\psi^{\phi}_{-,L}\rangle\langle\psi^{\phi}_{-,L}|\otimes|\Phi^-\rangle\langle\Phi^-|.\end{aligned} \tag{17}$$

It suffices for Alice and Bob to perform local measurements and use classical communication to determine if the logical Bell pair is $|\Phi^+\rangle$ or $|\Phi^-\rangle$. For instance, Alice and Bob would both measure in the eigenbasis of the logical X operator, and accept only the odd parity outcome. This odd parity outcome corresponds to a projection onto the state $|\Phi^-\rangle$, which reveals that a star photon has been captured into the memory qubits. In this case, we obtain the state

$$\rho'_{AB} = \left(\frac{1+\gamma}{2}\right)|\psi^{\phi}_{+,L}\rangle\langle\psi^{\phi}_{+,L}| + \left(\frac{1-\gamma}{2}\right)|\psi^{\phi}_{-,L}\rangle\langle\psi^{\phi}_{-,L}|. \tag{18}$$

This method can be extended to accommodate for multiple photon events, see Supplemental Materials for an example with two photons.

After projecting out the vacuum, we can use local measurements to extract information on ϕ and γ. The QFI for ϕ is $\gamma^2\epsilon$, and the QFI for γ is $\epsilon/(1-\gamma^2)$. The optimal measurement is non-unique for our case here; in the ideal case, local measurement is sufficient to saturate the quantum Cramer-Rao bound. Indeed, the local measurement basis $\frac{1}{\sqrt{2}}(|0_L\rangle \pm e^{i\theta}\,|1_L\rangle)_A \otimes \frac{1}{\sqrt{2}}(|0_L\rangle \pm |1_L\rangle)_B$ allows us to saturates the quantum Cramer-Rao bound, where θ is an adjustable phase. If we want to avoid applying a logical phase gate based on previous estimate, we could do this in a robust manner using geometric phases during the STIRAP stage. We can achieve this by changing the relative phase of the pump pulse $\Omega(t)$ and the single atom coupling g dynamically during the sequence, then a geometric phase will accumulate depending on the path in parameter space [34].

To optimally measure ϕ, we can adaptively adjust $\theta \to \pi/2 - \phi_{\mathrm{est}}$; to optimally measure γ, $\theta = -\phi_{\mathrm{est}}$, where ϕ_{est} is our best estimate of ϕ. If the QEC code is a stabiliser code, this measurement basis can furthermore be made to comprise of stabiliser states, by offseting the phase θ using geometric phase gates. This allows our scheme to be measured using any measurement protocol that measures in the stabiliser basis.

Physically, STIRAP has been implemented on many different platforms, including Rydberg atoms[35, 36], trapped ions [37, 38] semiconductor quantum dots [39], superconducting circuits [40] and etc. The metric for the quality of the atom-cavity system is the cooperativity $C = 2g^2/\kappa\eta$, which is the ratio of g to the cavity loss

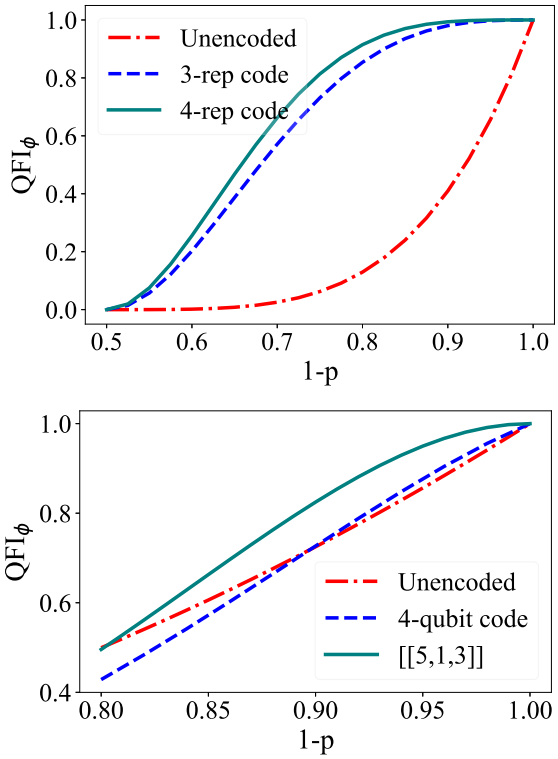

FIG. 4. For $\gamma = 1$, (top) the QFI for ϕ for the dephasing channel, when we use no encoding (red dotted-dashed line), the 3- and 4-repetition (blue dashed line and teal solid line); (bottom) the depolarising channel when we use the 4-qubit code [42] (blue dashed line) and the [[5,1,3]] error correction code (teal solid line).

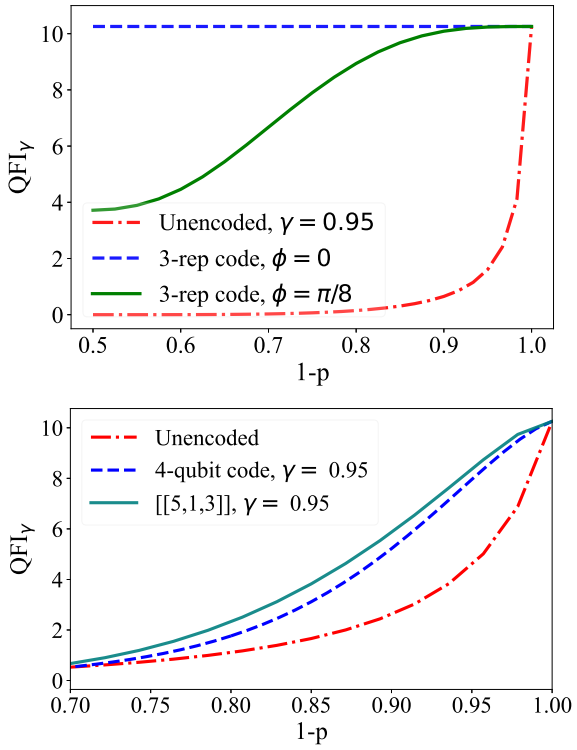

FIG. 5. For $\gamma = 0.95$, (top) the QFI for γ of the dephasing channel, when no encoding is used (red dotted-dashed line), and the 3-repetition code, when $\phi = 0$ (blue dashed line), and when $\phi = \pi/8$ (green solid line); (bottom) the depolarising channel when we use the 4-qubit code (blue dashed line) and the [[5,1,3]] error correction code (teal solid line).

rate κ, and the decay rate of the atom into non-cavity modes η. The potential for achieving high cooperativity gives cavity QED a central role in the development of high-fidelity quantum gates. A recent result reports a cooperativity $C = 299$ [41] for Rubidium atoms in a fibre cavity that is potentially compatible with our setup.

VI. QUANTUM ERROR CORRECTION

After the STIRAP interaction and the parity measurement, Alice and Bob share the quantum state ρ'_{AB} in Eq. (16), which is entangled over $2n$ qubits (they each hold n of them). We can calculate the QFI of ρ'_{AB} with respect to the signal that has been encoded with QEC. For an $[[n, k, d]]$ QEC code, n is the number of physical qubits, k is the number of logical qubits encoded, and d is the distance. The distance is the minimum number of physical errors it takes to change one logical codeword into another. Any QEC code with distance d can correct up to $t = \lfloor (d-1)/2 \rfloor$ errors [43], where $\lfloor \cdot \rfloor$ indicates the floor function.

The choice of which QEC code to use depends on various conditions, such as the number of available physical qubits, and the noise model. We now illustrate how our QEC-scheme performs when a dephasing and depolarising channel afflicts each qubit when n is small. Since n is small, the exact QFI can be calculated. We describe the dephasing channel as

$$\mathcal{E}_{\text{dephase}}[\rho] \to (1-p)\,\rho + p\sigma_z\rho\sigma_z^\dagger, \tag{19}$$

where σ_z is the phase-flip operator. Here $p = 1/2$ corresponds to the completely dephasing channel. The depolarising channel acting on each qubit can be written as

$$\mathcal{E}_{\text{depol}}(\rho) = (1-p)\rho + pI/2, \tag{20}$$

where $(1-p)$ is the probability that the transmission is noiseless, and with probability p the state is replaced by the completely mixed state.

In Fig. 4 we show the QFI of ϕ per photon received as a function of the noise strength p for the two noisy channels. In most physical systems, dephasing is the dominant noise type. The unprotected case which does not use QEC codes has a QFI of $(1-2p)^4$, which drops off quickly even when p is small. Evident in the top graph, a simple quantum repetition code provides a significant advantage

over the unprotected case for all values of dephasing. The logical states of the repetition codes are $|0_L\rangle = |+\rangle^{\otimes n}$ and $|1\rangle = |-\rangle^{\otimes n}$, $|\pm\rangle = (|0\rangle + |1\rangle)/\sqrt{2}$, and as n increases, the resilience against noise increases. In the limit of large n, we expect the curve to approach a step function where the QFI is preserved for up to $p < 0.5$. This is evident from the Chernoff bound (see below) since the phase-flip distance of the repetition code is n.

For the depolarising channel, the unprotected case without QEC has a QFI equal to $2(1-p)^4/(2-2p+p^2)$. Here, the [[5,1,3]] code is able to offer protection for values of p up to about 20%. This feature arises because of the favorable distance to length ratio of the [[5,1,3]] code.

In Fig. 5 we show the QFI of γ per photon received. Note that γ is a non-unitary parameter, and behaves differently from ϕ: the QFI can be preserved despite more than $t = (d-1)/2$ error occurring. For error numbers less than n, phase-flip errors put the state onto orthogonal and correctable subspaces. Surprisingly, if $\phi = 0$, the repetition code can preserve its QFI perfectly. There are two cases which leads to this phenomenon: if there are less than n phase flips, the state is put onto a correctable subspace, and the corresponding normalised state has the same QFI as the original state. When $2n$ phase-flip errors occur, the logical states $(|0_L\rangle|1_L\rangle \pm |1_L\rangle|0_L\rangle)/\sqrt{2}$ are eigenvectors of these errors with eigenvalues ± 1: the state is effectively invariant under the noise channel.

For $\phi \neq 0$, the advantage afforded is also significant; more importantly, one can adaptively change the adjustable phase so that the effective value of ϕ is close to 0 when the state is encoded.

For the depolarising channel, we see that the four-qubit code [42] with logical codewords $(|0000\rangle + |1111\rangle)/\sqrt{2}$ and $(|0011\rangle + |1100\rangle)/\sqrt{2}$ and the [[5,1,3]] QEC code also offers protection for a modest range of p.

To understand the behaviour of large quantum codes, now let us consider any noise model that introduces some error on each qubit independently with probability p. Now, let ϵ_{fail} denote the probability of having an uncorrectable error, where ϵ_{fail} is at most the probability of having at least $d/2$ errors. Using the Chernoff-Hoeffding bound for Bernoulli random variables [44], whenever $p < d/(2n)$, we have [45, 46]

$$\epsilon_{\text{fail}} \leq e^{-D(d/2n\|p)n}, \tag{21}$$

where $D(x\|y) = x\ln(x/y) + (1-x)\ln((1-x)/(1-y)$ denotes the Kullback-Leibler divergence. Note that ϵ_{fail} vanishes exponentially in n for small enough p. For large QEC codes, $d/(2n)$ asymptotes to a positive constant. By the quantum Gilbert-Varshamov bound [47–50], we know that if we use random QEC codes, we can have d/n approaching 0.1893 for large n. Hence, for our scheme such QEC codes can tolerate noise afflicting up to 9.4% of the qubits while preserving the QFI. This means that for $p < 0.094$, the QFI will be almost equal to that of when $p = 0$, if d and n are large enough.

If we have a noise model where memory qubits are randomly deleted, we can use permutation-invariant codes [51–53] for which deletion errors are equivalent to erasure errors [54, 55], and up to $O(\sqrt{n})$ deletions using n qubits can be corrected [54]. A noise model that randomly deletes and inserts separable states can also be corrected using permutation-invariant codes, because of the equivalence in the correctibility of deletion and separable insertion errors [56].

VII. DISCUSSIONS AND CONCLUSIONS

We have proposed a general framework for applying QEC to an imaging task, where the experimenter did not prepare the probe. In combination with pre-distributed entanglement, this allows us to protect the received signal from noise, thus enabling large-baseline optical interferometers that can out-perform what is feasible classically. By using STIRAP, we avoid noise sources such as amplitude damping that would hinder previous proposals. Although we cannot illuminate our objects for astronomical imaging, we can nonetheless perform super-resolution imaging beyond the diffraction limit [57–60]. This is because we preserve the phase information of the quantum state, and also use some prior structure of the astronomical sources. From this perspective, our work complements the currently active area of quantum super-resolution imaging research [57, 61–68].

We have entered the stage where quantum computers with tens – or soon hundreds – of qubits are becoming available. Much research effort has focused on using such noisy intermediate-scale quantum (NISQ) [69] devices to demonstrate capabilities that surpass classical computers. Here, we have proposed an application for such a NISQ device for imaging, where we protect the information encoded in the received starlight. For the dominant noise type—dephasing—we show that a significant advantage can be gained by using even a simple repetition code. For noise types (even adversarial) that corrupt up to a certain fraction of the qubits, we find the threshold —9.4%—for which the quantum Fisher information can be preserved. This threshold is significantly less stringent than that required for quantum computation. For pure dephasing, we can tolerate error rates up to 50%.

We anticipate that by leveraging on the theory of fault-tolerant quantum computation [33], our scheme can achieve a high QFI even with imperfect QEC operations. We will need in particular fault-tolerant syndrome extraction, using for instance the method of flag qubits [70], which only requires a modest overhead in the number of ancillary qubits. Namely, using any distance d stabilizer code, one only needs $d+1$ additional ancilla qubits.

Additionally, one could view the star as a source of preparing non-Clifford states, given that we have high-precision estimation of the phase and a stable source, e.g. in a satellite-based detection context.

VIII. ACKNOWLEDGEMENTS

ZH is supported by a Sydney Quantum Academy Postdoctoral Fellowship, and thanks Jonathan P. Dowling for inspiring this line of research. We thank Thomas Volz for his insightful discussions. G.K.B. acknowledges support from the Australian Research Council Centre of Excellence for Engineered Quantum Systems (Grant No. CE 170100009). Y.O. is supported by the Quantum Engineering Programme grant NRF2021-QEP2-01-P06, and also in part by NUS startup grants (R-263-000-E32-133 and R-263-000-E32-731), and the National Research Foundation, Prime Minister's Office, Singapore and the Ministry of Education, Singapore under the Research Centres of Excellence program.

[1] V. Giovannetti, S. Lloyd, and L. Maccone, Physical review letters **96**, 010401 (2006).
[2] V. Giovannetti, S. Lloyd, and L. Maccone, Nature photonics **5**, 222 (2011).
[3] J. W. Lichtman and J.-A. Conchello, Nature methods **2**, 910 (2005).
[4] C. A. Casacio, L. S. Madsen, A. Terrasson, M. Waleed, K. Barnscheidt, B. Hage, M. A. Taylor, and W. P. Bowen, Nature **594**, 201 (2021).
[5] A. R. Thompson, J. M. Moran, and G. W. Swenson, *Interferometry and synthesis in radio astronomy* (Springer Nature, 2017).
[6] A. Labeyrie, Astronomy and Astrophysics Supplement Series **118**, 517 (1996).
[7] P. Stee, F. Allard, M. Benisty, L. Bigot, N. Blind, H. Boffin, M. B. Fernandes, A. Carciofi, A. Chiavassa, O. Creevey, *et al.*, arXiv preprint arXiv:1703.02395 (2017).
[8] E. T. Khabiboulline, J. Borregaard, K. De Greve, and M. D. Lukin, Phys. Rev. Lett. **123**, 070504 (2019).
[9] B. M. Terhal, Rev. Mod. Phys. **87**, 307 (2015).
[10] S. Zhou, M. Zhang, J. Preskill, and L. Jiang, Nature communications **9**, 1 (2018).
[11] R. Demkowicz-Dobrzański, J. Czajkowski, and P. Sekatski, Phys. Rev. X **7**, 041009 (2017).
[12] Z. Huang, C. Macchiavello, and L. Maccone, Phys. Rev. A **94**, 012101 (2016).
[13] N. Shettell, W. J. Munro, D. Markham, and K. Nemoto, New Journal of Physics **23**, 043038 (2021).
[14] E. M. Kessler, I. Lovchinsky, A. O. Sushkov, and M. D. Lukin, Phys. Rev. Lett. **112**, 150802 (2014).
[15] W. Dür, M. Skotiniotis, F. Fröwis, and B. Kraus, Phys. Rev. Lett. **112**, 080801 (2014).
[16] T. Unden, P. Balasubramanian, D. Louzon, Y. Vinkler, M. B. Plenio, M. Markham, D. Twitchen, A. Stacey, I. Lovchinsky, A. O. Sushkov, M. D. Lukin, A. Retzker, B. Naydenov, L. P. McGuinness, and F. Jelezko, Phys. Rev. Lett. **116**, 230502 (2016).
[17] D. Layden, S. Zhou, P. Cappellaro, and L. Jiang, Phys. Rev. Lett. **122**, 040502 (2019).
[18] Y. Ouyang, N. Shettell, and D. Markham, IEEE Transactions on Information Theory **68**, 1809 (2022).
[19] Y. Ouyang and N. Rengaswamy, arXiv preprint arXiv:2007.02859 (2020).
[20] N. V. Vitanov, A. A. Rangelov, B. W. Shore, and K. Bergmann, Rev. Mod. Phys. **89**, 015006 (2017).
[21] D. Gottesman, T. Jennewein, and S. Croke, Phys. Rev. Lett. **109**, 070503 (2012).
[22] L. Mandel and E. Wolf, *Optical coherence and quantum optics* (Cambridge university press, 1995).
[23] M. E. Pearce, E. T. Campbell, and P. Kok, Quantum **1**, 21 (2017).
[24] E. T. Khabiboulline, J. Borregaard, K. De Greve, and M. D. Lukin, Phys. Rev. A **100**, 022316 (2019).
[25] S. L. Braunstein and C. M. Caves, Phys. Rev. Lett. **72**, 3439 (1994).
[26] I. Afnan, R. Banerjee, S. L. Braunstein, I. Brevik, C. M. Caves, B. Chakraborty, E. Fischbach, L. Lindblom, G. Milburn, S. Odintsov, *et al.*, Ann. Phys. **247**, 447 (1996).
[27] M. G. Paris, International Journal of Quantum Information **7**, 125 (2009).
[28] M. Jarzyna and R. Demkowicz-Dobrzański, Phys. Rev. Lett. **110**, 240405 (2013).
[29] S. Ragy, M. Jarzyna, and R. Demkowicz-Dobrzański, Phys. Rev. A **94**, 052108 (2016).
[30] P. Jessen, D. Haycock, G. Klose, G. Smith, I. Deutsch, and G. Brennen, Quantum Information & Computation **1**, 20 (2001).
[31] G. S. Vasilev, A. Kuhn, and N. V. Vitanov, Phys. Rev. A **80**, 013417 (2009).
[32] X. Zhou, D. W. Leung, and I. L. Chuang, Phys. Rev. A **62**, 052316 (2000).
[33] E. T. Campbell, B. M. Terhal, and C. Vuillot, Nature **549**, 172 (2017).
[34] D. Møller, L. B. Madsen, and K. Mølmer, Phys. Rev. A **75**, 062302 (2007).
[35] T. Cubel, B. K. Teo, V. S. Malinovsky, J. R. Guest, A. Reinhard, B. Knuffman, P. R. Berman, and G. Raithel, Phys. Rev. A **72**, 023405 (2005).
[36] M. Saffman, T. G. Walker, and K. Mølmer, Rev. Mod. Phys. **82**, 2313 (2010).
[37] N. Timoney, I. Baumgart, M. Johanning, A. Varón, M. B. Plenio, A. Retzker, and C. Wunderlich, Nature **476**, 185 (2011).
[38] S. C. Webster, S. Weidt, K. Lake, J. J. McLoughlin, and W. K. Hensinger, Phys. Rev. Lett. **111**, 140501 (2013).
[39] T. S. Koh, S. Coppersmith, and M. Friesen, Proceedings of the National Academy of Sciences **110**, 19695 (2013).
[40] J.-Q. You and F. Nori, Nature **474**, 589 (2011).
[41] S. Garcia, F. Ferri, J. Reichel, and R. Long, Optics Express **28**, 15515 (2020).
[42] D. W. Leung, M. A. Nielsen, I. L. Chuang, and Y. Yamamoto, Phys. Rev. A **56**, 2567 (1997).
[43] J. Roffe, Contemporary Physics **60**, 226 (2019).
[44] W. Hoeffding, Amer. Stat. Assoc, J. **58**, 13 (1963).
[45] H. Chernoff *et al.*, The Annals of Mathematical Statistics **23**, 493 (1952).
[46] M. Okamoto, Annals of the institute of Statistical Mathematics **10**, 29 (1959).

[47] K. Feng and Z. Ma, IEEE Transactions on Information Theory **50**, 3323 (2004).
[48] Y. Ma, Journal of Mathematical Analysis and Applications **340**, 550 (2008).
[49] L. Jin and C. Xing, in *IEEE International Symposium on Information Theory Proceedings (ISIT)* (2011) pp. 455–458.
[50] Y. Ouyang, IEEE Transactions on Information Theory **60**, 3117 (2014).
[51] Y. Ouyang, Phys. Rev. A **90**, 062317 (2014), 1302.3247.
[52] Y. Ouyang and J. Fitzsimons, Phys. Rev. A **93**, 042340 (2016).
[53] Y. Ouyang, Linear Algebra and its Applications **532**, 43 (2017).
[54] Y. Ouyang, in *2021 IEEE International Symposium on Information Theory (ISIT)* (2021) pp. 1499–1503.
[55] T. Shibayama and M. Hagiwara, *2021 IEEE International Symposium on Information Theory (ISIT)*, , 1493 (2021).
[56] T. Shibayama and Y. Ouyang, in *2021 IEEE Information Theory Workshop (ITW)* (IEEE, 2021) pp. 1–6.
[57] M. Tsang, Contemporary Physics **60**, 279 (2019).
[58] R. Nair and M. Tsang, Phys. Rev. Lett. **117**, 190801 (2016).
[59] C. Lupo, Z. Huang, and P. Kok, Phys. Rev. Lett. **124**, 080503 (2020).
[60] Z. Huang and C. Lupo, Phys. Rev. Lett. **127**, 130502 (2021).
[61] Z. Huang, C. Lupo, and P. Kok, PRX Quantum **2**, 030303 (2021).
[62] M. P. Backlund, Y. Shechtman, and R. L. Walsworth, Phys. Rev. Lett. **121**, 023904 (2018).
[63] Z. Yu and S. Prasad, Phys. Rev. Lett. **121**, 180504 (2018).
[64] C. Napoli, S. Piano, R. Leach, G. Adesso, and T. Tufarelli, Phys. Rev. Lett. **122**, 140505 (2019).
[65] W.-K. Tham, H. Ferretti, and A. M. Steinberg, Phys. Rev. Lett. **118**, 070801 (2017).
[66] M. Parniak, S. Borówka, K. Boroszko, W. Wasilewski, K. Banaszek, and R. Demkowicz-Dobrzański, Phys. Rev. Lett. **121**, 250503 (2018).
[67] J. Hassett, T. Malhorta, M. Alonso, R. Boyd, S. H. Rafsanjani, and A. Vamivakas, in *Laser Science* (Optical Society of America, 2018) pp. JW4A–124.
[68] Y. Zhou, J. Yang, J. D. Hassett, S. M. H. Rafsanjani, M. Mirhosseini, A. N. Vamivakas, A. N. Jordan, Z. Shi, and R. W. Boyd, Optica **6**, 534 (2019).
[69] J. Preskill, Quantum **2**, 79 (2018).
[70] R. Chao and B. W. Reichardt, PRX Quantum **1**, 010302 (2020).

Supplemental Materials

IX. QFI OF THE UNPROTECTED STATE

In this section we derive the QFI associated with noise introduced by the environment in the unencoded case. Consider the case where there is at most a single photon arriving on the two sites, where $\epsilon \ll 1$. We can describe the optical state by the density matrix

$$\begin{aligned}\rho_\star \approx &(1-\epsilon)\left|\text{vac},\text{vac}\right\rangle\left\langle\text{vac},\text{vac}\right|_{A_1B_1} + \\ &\epsilon\left(\frac{1+\gamma}{2}\right)\left|\psi_+^\phi\right\rangle\left\langle\psi_+^\phi\right| + \epsilon\left(\frac{1-\gamma}{2}\right)\left|\psi_-^\phi\right\rangle\left\langle\psi_-^\phi\right|\end{aligned} \tag{S1}$$

where $|\psi_\pm^\phi\rangle = 1/\sqrt{2}(|1_p\rangle_{A_1}|\text{vac}\rangle_{B_1} \pm e^{i\phi}|\text{vac}\rangle_{A_1}|1_p\rangle_{B_1})$, here the subscript p denotes a single photonic Fock state.

In the noiseless scenario, the QFI and SLD for γ are:

$$\begin{aligned}\text{QFI}_\gamma =&\frac{\epsilon}{1-\gamma^2},\\ \text{SLD}_\gamma =&\frac{-1}{1-\gamma}\left|\psi_-^\phi\right\rangle\left\langle\psi_-^\phi\right| + \frac{1}{\gamma+1}\left|\psi_+^\phi\right\rangle\left\langle\psi_+^\phi\right|.\end{aligned} \tag{S2}$$

And for ϕ

$$\begin{aligned}\text{QFI}_\phi &= \gamma^2\epsilon,\\ \text{SLD}_\phi &= i\gamma(\left|\psi_+^\phi\right\rangle\left\langle\psi_+^\phi\right| - \left|\psi_-^\phi\right\rangle\left\langle\psi_-^\phi\right|).\end{aligned} \tag{S3}$$

A. Amplitude damping

In the unencoded case, if the ground-excited state is used to store the information, the state of the memory qubit is predominantly subjected to dephasing and amplitude damping noise. We begin with the memory state

$$\begin{aligned}\rho_{AB} =&(1-\epsilon)\left|g,g\right\rangle\left\langle g,g\right|_{AB}+\\ &\epsilon\left(\frac{1+\gamma}{2}\right)\left|\psi'^{\,\phi}_{+}\right\rangle\left\langle\psi'^{\,\phi}_{+}\right|+\\ &\epsilon\left(\frac{1-\gamma}{2}\right)\left|\psi'^{\,\phi}_{-}\right\rangle\left\langle\psi'^{\,\phi}_{-}\right|,\end{aligned}\tag{S4}$$

$\left|\psi'^{\,\phi}_{\pm}\right\rangle = (\left|g,e\right\rangle_{AB} \pm e^{i\phi}\left|e,g\right\rangle_{AB})/\sqrt{2}$.

In the basis $|g,e\rangle$, the Amplitude damping channel (ADC) has Krauss operators

$$D_0 = \begin{pmatrix} 1 & 0 \\ 0 & \sqrt{1-\eta} \end{pmatrix}, \quad D_1 = \begin{pmatrix} 0 & \sqrt{\eta} \\ 0 & 0 \end{pmatrix}.\tag{S5}$$

After applying the ADC, the density matrix becomes

$$\begin{aligned}\mathcal{E}[\rho_{AB}] \to 1-&\epsilon(1-\eta)\left|g,g\right\rangle+\\ &(1-\eta)\epsilon\left(\frac{1+\gamma}{2}\right)\left|\psi'^{\,\phi}_{+}\right\rangle\left\langle\psi'^{\,\phi}_{+}\right|+\\ &(1-\eta)\epsilon\left(\frac{1-\gamma}{2}\right)\left|\psi'^{\,\phi}_{-}\right\rangle\left\langle\psi'^{\,\phi}_{-}\right|.\end{aligned}\tag{S6}$$

That is, if the damping strength η is equal on Alice and Bob's sites, then this is equivalent to reducing ϵ by a factor of $(1-\eta)$, and hence the QFI for both parameters is reduced by a factor $(1-\eta)$.

X. DEPHASING

We now analyse the dephasing channel, where phase errors σ_z occurs with probability p. In our notation, $p = 1/2$ corresponds to a completely dephasing channel that acts on a single-qubit state ρ

$$\mathcal{E}[\rho] \to (1-p)\,\rho_\star + p\sigma_z\rho_\star\sigma_z^\dagger.\tag{S7}$$

Assuming the qubits held by Alice and Bob have the same dephasing parameter p, the QFI is

$$\begin{aligned}\mathrm{QFI}_\phi &= (1-2p)^4\gamma^2\epsilon\\ \mathrm{QFI}_\gamma &= \frac{(1-2p)^4\epsilon}{1-\gamma^2(1-2p)^4}.\end{aligned}\tag{S8}$$

XI. FI AND QFI BOUNDS

After QEC, we have the state

$$\rho_\theta = (1-\epsilon_{\text{fail}})\rho_0 + \epsilon_{\text{fail}}\sigma,\tag{S9}$$

where ρ_0 is the ideal state, and σ is some noisy state that was not correctable. Let L be an observable that we want to implement. Then we want

$$\mathrm{Tr}(\rho_\theta L^2) - \mathrm{Tr}(\rho_\theta L)^2.\tag{S10}$$

We use the error propagation formula to find that the variance of the parameter of interest is

$$\mathrm{Var}(\hat{\theta}) = \frac{\mathrm{Tr}(\rho_\theta L^2) - \mathrm{Tr}(\rho_\theta L)^2}{\left|\frac{\partial}{\partial\theta}\mathrm{Tr}(\rho_\theta L)\right|^2}. \tag{S11}$$

XII. ACHIEVABLE BOUNDS

An explicit form of the optimal estimator for the parameter θ is given by [S27]

$$\hat{O}_\theta = \theta\mathbb{1} + \frac{\hat{L}_\theta}{J(\theta)} \tag{S12}$$

where L_θ is the SLD and $J(\theta)$ is the QFI. This results in

$$\langle O_\theta\rangle = \theta, \qquad \langle\Delta O\rangle^2 = 1/J(\theta). \tag{S13}$$

For a particular observable $\hat{X}$, by error propagation, the achievable variance is

$$(\Delta\theta)^2 = \frac{\mathrm{Tr}[\rho_\theta X^2] - \mathrm{Tr}[\rho_\theta X]^2}{|\frac{\partial}{\partial\theta}\mathrm{Tr}[X\rho_\theta]|^2}. \tag{S14}$$

A. Achievable bounds for an optimal observable based on the SLD - most reasonable noise channels

Based on detection per photon (normalised by $1/\epsilon$), one optimal observable based on the SLD of ϕ is

$$\hat{P} = (|\psi_+^\alpha\rangle\langle\psi_+^\alpha| - |\psi_-^\alpha\rangle\langle\psi_-^\alpha|), \tag{S15}$$

where α is an adjustable phase. Setting $\hat{P} = X$ in (S14), we find that the numerator of (S14) is upper bounded by the norm of P, where $\|P\|^2 = 1$.

For the denominator, we start with

$$\begin{aligned}\rho' P =&(1-\epsilon_{\text{fail}})\rho_0 P + \epsilon_{\text{fail}}\sigma P\\ \langle\rho' P\rangle =&(1-\epsilon_{\text{fail}})\gamma\cos(\alpha+\phi) + \langle\epsilon_{\text{fail}}\sigma P\rangle\end{aligned} \tag{S16}$$

where the first term stems from the fact that, if the error is correctable, the state can be returned to being ρ_0, and $\rho = (\frac{1+\gamma}{2})|\psi_+^\phi\rangle\langle\psi_+^\phi| + (\frac{1-\gamma}{2})|\psi_-^\phi\rangle\langle\psi_-^\phi|$.

From the reverse triangle inequality, $|x-y| \geq \big||x|-|y|\big|$, we have

$$|\partial_\phi\langle\rho' P\rangle| \geq \gamma(1-\epsilon_{\text{fail}})|\sin(\alpha+\phi)| - \epsilon_{\text{fail}}|\partial_\phi\langle\sigma P\rangle|. \tag{S17}$$

The magnitude of $\langle\sigma P\rangle \leq \gamma$, because P is a projector onto real-component of the off-diagonal components. For most "reasonable" noise channels (i.e. most of the physical noise types considered in the QEC literature), the dependence of $|\langle\sigma P\rangle|$ on ϕ should not be larger than that of $\langle\rho_0 P\rangle$, which means that the derivative has magnitude at most equal equal to $\sin(\beta+\phi)]$, where β can be in general not equal to α. Assuming $\epsilon_{\text{fail}} \leq 1/2$, when we adjust the phase in the measurement α such that $\alpha - \phi = \pi/2$, we have

$$|\langle\rho' P\rangle| \geq \gamma(1-2\epsilon_{\text{fail}})^2, \tag{S18}$$

and therefore

$$(\Delta\phi)^2 \leq \frac{1}{\gamma^2(1-2\epsilon_{\text{fail}})^2}. \tag{S19}$$

In fact, for channels such as depolarising, dephasing and amplitude damping, any noisy component of the state has no off-diagonal components, where $\langle\sigma P\rangle = 0$. For these cases, we achieve $(\Delta\phi)^2 \leq 1/\gamma^2(1-\epsilon_{\text{fail}})^2$.

B. Achievable bounds for an observable based on local measurements - most reasonable noise channels

Now, consider the separable observable, where the state is projected onto the basis $|\pm^\alpha\rangle_A \otimes |\pm\rangle_B = \frac{1}{\sqrt{2}}(|0\rangle \pm e^{i\alpha}|1\rangle)_A \otimes \frac{1}{\sqrt{2}}(|0\rangle \pm |1\rangle)_B$, and consider the observable

$$P_{\text{sep}} = |+^\alpha,+\rangle\langle+^\alpha,+| + |-^\alpha,+\rangle\langle-^\alpha,+| - (|+^\alpha,-\rangle\langle+^\alpha,-| + |-^\alpha,+\rangle\langle-^\alpha,+|). \tag{S20}$$

We have $\|P_{\text{sep}}\|^2 = 1$. Note that

$$\begin{aligned}\rho' P_{\text{sep}} =& (1-\epsilon_{\text{fail}})\rho_0 P_{\text{sep}} + \epsilon_{\text{fail}}\sigma P_{\text{sep}} \\ \langle\rho' P_{\text{sep}}\rangle =& (1-\epsilon_{\text{fail}})\gamma\cos(\alpha+\phi) + \langle\epsilon_{\text{fail}}\sigma P_{\text{sep}}\rangle\,.\end{aligned} \tag{S21}$$

Similarly as before, we obtain an upper bound for $(\Delta\phi)^2$.

XIII. HIGHER PHOTON CONTRIBUTIONS

In reality, the state received from the star is thermal. Therefore the probability of having more than 1 photon is non zero. Since the mean photon number is usually slow, we truncate the term at two photons; in this section, we work out the two-photon states in the Fock basis.

The covariance matrix in the basis $\{a, a^\dagger, b, b^\dagger\}$ (a (b) being the mode at the collector held by Alice (Bob) is

$$\Sigma = \begin{pmatrix} 0 & \frac{\epsilon}{2}+\frac{1}{2} & 0 & \frac{1}{2}\gamma\epsilon\exp(i\phi) \\ \frac{\epsilon}{2}+\frac{1}{2} & 0 & \frac{1}{2}\gamma\epsilon\exp(-i\phi) & 0 \\ 0 & \frac{1}{2}\gamma\epsilon\exp(-i\phi) & 0 & \frac{\epsilon}{2}+\frac{1}{2} \\ \frac{1}{2}\gamma\epsilon\exp(i\phi) & 0 & \frac{\epsilon}{2}+\frac{1}{2} & 0 \end{pmatrix} \tag{S22}$$

given ϵ is the mean total photon number, and γ, θ as per defined above.

This state is diagonalisable with a phase shifter and a 50:50 BS:

$$S = \frac{1}{\sqrt{2}}\begin{pmatrix} 1 & 0 & 1 & 0 \\ 0 & 1 & 0 & 1 \\ 1 & 0 & -1 & 0 \\ 0 & 1 & 0 & -1 \end{pmatrix}\begin{pmatrix} 1 & 0 & 0 & 0 \\ 0 & 1 & 0 & 0 \\ 0 & 0 & \exp(-i\alpha) & 0 \\ 0 & 0 & 0 & \exp(i\alpha) \end{pmatrix}. \tag{S23}$$

We have

$$\Sigma' = S\Sigma S^T = \begin{pmatrix} 0 & \frac{1}{2}(\gamma\epsilon+\epsilon+1) & 0 & 0 \\ \frac{1}{2}(\gamma\epsilon+\epsilon+1) & 0 & 0 & 0 \\ 0 & 0 & 0 & \frac{1}{2}(-\gamma\epsilon+\epsilon+1) \\ 0 & 0 & \frac{1}{2}(-\gamma\epsilon+\epsilon+1) & 0 \end{pmatrix}. \tag{S24}$$

We will need the Hermitian conjugate of S

$$S^\dagger = \frac{1}{\sqrt{2}}\begin{pmatrix} 1 & 0 & 1 & 0 \\ 0 & 1 & 0 & 1 \\ e^{i\alpha} & 0 & -e^{i\alpha} & 0 \\ 0 & e^{-i\alpha} & 0 & -e^{-i\alpha} \end{pmatrix} \tag{S25}$$

because a thermal state in the number basis is written as

$$\rho_G = S^\dagger\left(\bigotimes^n \rho_n\right)S. \tag{S26}$$

This means that for a two-mode thermal state, we have

$$\begin{aligned}
\rho &= \rho_a \otimes \rho_b, \\
\rho_a &= \sum_i \frac{1}{n_a+1}\left(\frac{n_a}{n_a+1}\right)^i |i\rangle\langle i|, \qquad n_a = \frac{1}{2}(\epsilon+\gamma\epsilon) \\
\rho_b &= \sum_j \frac{1}{n_b+1}\left(\frac{n_b}{n_b+1}\right)^j |j\rangle\langle j|, \qquad n_b = \frac{1}{2}(\epsilon-\gamma\epsilon) \\
\rho_a \otimes \rho_b &= \sum_{i,j} \frac{1}{(n_a+1)(n_b+1)}\left(\frac{n_a}{n_a+1}\right)^i \left(\frac{n_b}{n_b+1}\right)^j \frac{(a'^\dagger_1)^i}{i!}\frac{(a'^\dagger_2)^j}{j!}|0,0\rangle\langle 0,0|(a'_1)^i(a'_2)^j.
\end{aligned} \tag{S27}$$

To invert the diagonalising operation, the operators in Eq (S27) should transform as

$$\begin{aligned}
a'^\dagger_1 &\to \frac{1}{\sqrt{2}}(a^\dagger_1 + a^\dagger_2 e^{i\phi}) \\
a'^\dagger_2 &\to \frac{1}{\sqrt{2}}(a^\dagger_1 - a^\dagger_2 e^{i\phi}).
\end{aligned} \tag{S28}$$

Now denote $p(i,j)$ to have i and j number of photons from the modes held by Alice and Bob after diagonalising the covariance matrix. Let us separate the terms. For a total of 0 photons, we have

$$p(0,0) = \frac{1}{(n_a+1)(n_b+1)}. \tag{S29}$$

With one photon shared between either modes, we have

$$\begin{aligned}
p(1) = p(1,0) + p(0,1) =& \frac{1}{(n_a+1)(n_b+1)}\left(\frac{n_a}{n_a+1}\right)\frac{(a^\dagger_1 + e^{i\phi}a^\dagger_2)}{2}|0,0\rangle\langle 0,0|(a_1 + e^{-i\phi}a_2) + \\
& \frac{1}{(n_a+1)(n_b+1)}\left(\frac{n_b}{n_b+1}\right)\frac{(a^\dagger_1 - a^\dagger_2 e^{i\phi})}{2}|0,0\rangle\langle 0,0|(a_1 - a_2 e^{i\phi}) \\
=& \frac{1}{(n_a+1)(n_b+1)}\frac{1}{2}\left(\frac{n_a}{n_a+1}\right)|\psi^\phi_+\rangle\langle\psi^\phi_+| + \frac{1}{(n_a+1)(n_b+1)}\frac{1}{2}\left(\frac{n_b}{n_b+1}\right)|\psi^\phi_-\rangle\langle\psi^\phi_-|.
\end{aligned} \tag{S30}$$

Now, for the two-photon case, we have $i=1, j=1$, $i=2, j=0$, or $i=0, j=2$.

$$\begin{aligned}
p(2) =& p(1,1) + p(2,0) + p(0,2) \\
=& \frac{1}{(n_a+1)(n_b+1)}\left(\frac{n_a}{n_a+1}\right)\left(\frac{n_b}{n_b+1}\right)(a'^\dagger_1)(a'^\dagger_2)|0,0\rangle\langle 0,0|(a'_1)(a'_2) + \\
& \frac{1}{(n_a+1)(n_b+1)}\left(\frac{n_a}{n_a+1}\right)^2\frac{(a'^\dagger_1)^2}{2!}|0,0\rangle\langle 0,0|(a'_1)^2 + \frac{1}{(n_a+1)(n_b+1)}\left(\frac{n_b}{n_b+1}\right)^2\frac{(a'^\dagger_2)^2}{2!}|0,0\rangle\langle 0,0|(a'_2)^2.
\end{aligned} \tag{S31}$$

We evaluate the following expression,

$$\begin{aligned}
&(a'^{\dagger}_1)(a'^{\dagger}_2)\left|0,0\right\rangle\left\langle 0,0\right|(a'_1)(a'_2)\\
=&\frac{1}{4}(a_1^{\dagger}+a_2^{\dagger}e^{i\phi})(a_1^{\dagger}-a_2^{\dagger}e^{i\phi})\left|0,0\right\rangle\left\langle 1,1\right|(a_1+a_2e^{-i\phi})(a_1-a_2e^{-i\phi})\\
=&\frac{1}{4}(a_1^{\dagger 2}-e^{i2\phi}a_2^{\dagger 2})\left|0,0\right\rangle\left\langle 0,0\right|(a_1^2-e^{-i2\phi}a_2^2)\\
=&\frac{(\left|2,0\right\rangle-e^{i2\phi}\left|0,2\right\rangle)}{\sqrt{2}}\frac{(\left\langle 2,0\right|-e^{-i2\phi}\left\langle 0,2\right|)}{\sqrt{2}}\\
=&\left|\Psi_0^2\right\rangle\left\langle\Psi_0^2\right|. \qquad \text{(S32)}
\end{aligned}$$

For the $i=2, j=0$ term,

$$\begin{aligned}
&\frac{(a'^{\dagger}_1)^2}{2!}\left|0,0\right\rangle\left\langle 0,0\right|(a'_1)^2\\
=&\frac{1}{2!}\frac{1}{2}(a_1^{\dagger}+a_2^{\dagger}e^{i\phi})^2\left|0,0\right\rangle\left\langle 0,0\right|\frac{1}{2}(a_1+a_2e^{-i\phi})^2\\
=&\frac{1}{16}(a_1^{\dagger 2}+2a_1^{\dagger}a_2^{\dagger}e^{i\phi}+a_2^{\dagger 2}e^{i2\phi})\left|0,0\right\rangle\left\langle 0,0\right|(c.c)\\
=&\frac{1}{16}(\sqrt{2}\left|2,0\right\rangle+2e^{i\phi}1,1+\sqrt{2}e^{i2\phi}\left|0,2\right\rangle)\otimes c.c\\
=&\frac{1}{2}\times\frac{(\left|2,0\right\rangle+\sqrt{2}e^{i\phi}\left|1,1\right\rangle+e^{i2\phi}\left|0,2\right\rangle)}{2}\otimes c.c\\
=&\frac{1}{2}\left|\Psi_+^2\right\rangle\left\langle\Psi_+^2\right|. \qquad \text{(S33)}
\end{aligned}$$

Likewise for the $i=0, j=2$ term, we will have

$$\begin{aligned}
&\frac{(a'^{\dagger}_2)^2}{2!}\left|0,0\right\rangle\left\langle 0,0\right|(a'_2)^2\\
&=\frac{1}{2}\times\frac{(\left|2,0\right\rangle-\sqrt{2}e^{i\phi}\left|1,1\right\rangle+e^{i2\phi}\left|0,2\right\rangle)}{2}\otimes h.c.\\
=&\frac{1}{2}\left|\Psi_-^2\right\rangle\left\langle\Psi_-^2\right|. \qquad \text{(S34)}
\end{aligned}$$

Overall, the two-photon contributions are

$$\begin{aligned}
p(2)=&\frac{1}{(n_a+1)(n_b+1)}\left(\frac{n_a}{n_a+1}\right)\left(\frac{n_b}{n_b+1}\right)\left|\Psi_0^2\right\rangle\left\langle\Psi_0^2\right|+\\
&\frac{1}{(n_a+1)(n_b+1)}\left(\frac{n_a}{n_a+1}\right)^2\frac{1}{2}\left|\Psi_+^2\right\rangle\left\langle\Psi_+^2\right|+\frac{1}{(n_a+1)(n_b+1)}\left(\frac{n_b}{n_b+1}\right)^2\frac{1}{2}\left|\Psi_-^2\right\rangle\left\langle\Psi_-^2\right|. \qquad \text{(S35)}
\end{aligned}$$

XIV. MODIFIED HAMILTONIAN DUE TO MULTIPLE PHOTONS

Given n photons in the cavity, the full STIRAP Hamiltonian is

$$\begin{aligned}
H_{\text{stirap}}=&\omega_0\left|e\right\rangle\left\langle e\right|+\omega_c a^{\dagger}a+\\
&\Omega e^{-i\omega_L t}\left|e\right\rangle\left\langle 1\right|+\Omega^* e^{i\omega_L t}\left|1\right\rangle\left\langle e\right|+\\
&ga\left|0\right\rangle\left\langle e\right|+g^* a^{\dagger}\left|e\right\rangle\left\langle 0\right|. \qquad \text{(S36)}
\end{aligned}$$

In the rotating wave approximation $e^{-i\theta a^\dagger a} a e^{i\theta a^\dagger a} = e^{i\theta} a$,

$$\begin{aligned} H_I &= U_c^\dagger H U_c - H_c, \\ H_c &= \omega_c a^\dagger a + \omega_L \left|e\right\rangle \left\langle e\right|, \\ U_c &= e^{-i\omega_c a^\dagger a t} e^{-i\omega_L t \left|e\right\rangle\left\langle e\right|} \\ H_I &= -\Delta \left|e\right\rangle \left\langle e\right| + \Omega \left|e\right\rangle \left\langle 1\right| + \Omega^* \left|1\right\rangle \left\langle e\right| + g a \left|0\right\rangle \left\langle e\right| + g^* a^\dagger \left|e\right\rangle \left\langle 0\right|, \end{aligned} \tag{S37}$$

where $\Delta = \omega_L - \omega_0$. The last two terms connect pairs of bases with the same excitation number, i.e. $|g, n\rangle \rightleftharpoons |e, n-1\rangle$. This means that the Hamiltonian can be written as a direct sum in the basis

$$\{|1, n-1\rangle, |e, n-1\rangle, |0, n\rangle\}. \tag{S38}$$

We have ($H_{i,j} = \langle i|H|j\rangle$)

$$\begin{aligned} H^{(n)} &= \begin{pmatrix} \langle 1,n-1|H_{\text{stirap}}|1,n-1\rangle & \langle 1,n-1|H_{\text{stirap}}|e,n-1\rangle & \langle 1,n-1|H_{\text{stirap}}|0,n\rangle \\ \langle e,n-1|H_{\text{stirap}}|1,n-1\rangle & \langle e,n-1|H_{\text{stirap}}|e,n-1\rangle & \langle e,n-1|H_{\text{stirap}}|0,n\rangle \\ \langle 0,n|H_{\text{stirap}}|1,n-1\rangle & \langle 0,n|H_{\text{stirap}}|e,n-1\rangle & \langle 0,n|H_{\text{stirap}}|0,n\rangle \end{pmatrix} \\ &= \begin{pmatrix} 0 & \Omega^* & 0 \\ \Omega & -\Delta & g\sqrt{n} \\ 0 & g^*\sqrt{n} & 0 \end{pmatrix}. \end{aligned}$$

If the transfer unitary is perfect, the initial state turns into (with some phase difference, which we will observe numerically)

$$\begin{aligned} \left|0,0\right\rangle_A \left|0,2\right\rangle_B &\to \left|0,0\right\rangle_A \left|1,1\right\rangle_B \\ \left|0,1\right\rangle_A \left|0,1\right\rangle_B &\to \left|1,0\right\rangle_A \left|1,0\right\rangle_B. \end{aligned} \tag{S39}$$

Therefore if our initial state is

$$\begin{aligned} &\left|0\right\rangle_A \left|0\right\rangle_B \otimes \frac{1}{2}(\left|2,0\right\rangle + \sqrt{2} e^{i\phi} \left|1,1\right\rangle + e^{i2\phi} \left|0,2\right\rangle) \\ &\quad = \frac{1}{2} \left|0,2\right\rangle_A \left|0,0\right\rangle_B + \frac{1}{\sqrt{2}} e^{i\phi} \left|0,1\right\rangle_A \left|0,1\right\rangle_B + \frac{1}{2} e^{i2\phi} \left|0,0\right\rangle_A \left|0,2\right\rangle_b \end{aligned} \tag{S40}$$

then STIRAP takes it to the state

$$\to \frac{1}{2} \left|1,1\right\rangle_A \left|0,0\right\rangle_B + \frac{1}{\sqrt{2}} e^{i(\phi+\delta)} \left|1,0\right\rangle_A \left|1,0\right\rangle_B + \frac{1}{2} e^{i2\phi} \left|0,0\right\rangle_A \left|1,1\right\rangle_B \tag{S41}$$

We observe an additional relative phase on the $|1,0\rangle\,|1,0\rangle$ term, due to the dispersive coupling of the atom to the cavity in the presence of an additional photon.

Now, we are faced with the task of distinguishing between the different cases without perturbing the encoded phase information. Using the subscripts l to denote levels of an atomic system and p for photonic Fock states. These are the three states:

a. No photon has arrived:

$$\left|0_l, 0_p\right\rangle_A \left|0_l, 0_p\right\rangle_B. \tag{S42}$$

b. A single photon has arrived:

$$\frac{1}{\sqrt{2}}(\left|1_l, 0_p\right\rangle_A \left|0_l, 0_p\right\rangle_B \pm e^{i\phi} \left|0_l, 0_p\right\rangle_A \left|1_l, 0_p\right\rangle_B). \tag{S43}$$

c. Two photons have arrived:

$$
\begin{aligned}
|\psi_1\rangle &= \frac{1}{\sqrt{2}}(|1_l,1_p\rangle_A\,|0_l,0_p\rangle_B - e^{i2\phi}\,|0_l,0_p\rangle_A\,|1_l,1_p\rangle_B)\\
|\psi_2\rangle &\to \frac{1}{2}\,|1_l,1_p\rangle_A\,|0_l,0_p\rangle_B + \frac{1}{\sqrt{2}}e^{i(\phi+\delta)}\,|1_l,0_p\rangle_A\,|1_l,0_p\rangle_B + \frac{1}{2}e^{i2\phi}\,|0_l,0_p\rangle_A\,|1_l,1_p\rangle_B\\
|\psi_3\rangle &\to \frac{1}{2}\,|1_l,1_p\rangle_A\,|0_l,0_p\rangle_B - \frac{1}{\sqrt{2}}e^{i(\phi+\delta)}\,|1_l,0_p\rangle_A\,|1_l,0_p\rangle_B + \frac{1}{2}e^{i2\phi}\,|0_l,0_p\rangle_A\,|1_l,1_p\rangle_B\,.
\end{aligned}
\tag{S44}
$$

If we perform parity checks on the memory qubits and the cavity photon states (which can be achieved by using another auxilliary atom). We assume the Bell pairs $|\Phi^+\rangle$ are shared between Alice and Bob, where the subscript denotes which system they are paired with. For example,

$$
|1_l\rangle_A\,|0_l\rangle_B\,|\Phi_l^+\rangle \overset{2\times\mathrm{CZ}}{\to} |1_l\rangle_A\,|0_l\rangle_B\,|\Phi_l^-\rangle \tag{S45}
$$

denotes that 2 CZ gates (one on Alice and one of Bob's side) are applied, where the control qubits are in state $|1_l\rangle_A\,|0_l\rangle_B$, and the target qubits are in state $|\Phi_l^+\rangle$.

For the zero photon case:

$$
(|0_l,0_p\rangle_A\,|0_l,0_p\rangle_B)\,|\Phi_l^+\rangle\,|\Phi_p^+\rangle \overset{4\times\mathrm{CZ}}{\to} (|0_l,0_p\rangle_A)\,|0_l,0_p\rangle_B)\,|\Phi_l^+\rangle\,|\Phi_p^+\rangle\,. \tag{S46}
$$

For the single-photon case:

$$
(|1_l,0_p\rangle_A\,|0_l,0_p\rangle_B\,,|0_l,0_p\rangle_A\,|0_l,1_p\rangle_B)\,|\Phi_l^+\rangle\,|\Phi_p^+\rangle \overset{4\times\mathrm{CZ}}{\to} (|1_l,0_p\rangle_A\,|0_l,0_p\rangle_B\,,|0_l,0_p\rangle_A\,|0_l,1_p\rangle_B)\,|\Phi_l^-\rangle\,|\Phi_p^+\rangle\,. \tag{S47}
$$

For the two-photon case:

$$
(|1_l,1_p\rangle_A\,|0_l,0_p\rangle_B\,,|0_l,0_p\rangle_A\,|1_l,1_p\rangle_B)\,|\Phi_l^+\rangle\,|\Phi_p^+\rangle \overset{4\times\mathrm{CZ}}{\to} (|1_l,1_p\rangle_A\,|0_l,0_p\rangle_B\,,|0_l,0_p\rangle_A\,|1_l,1_p\rangle_B)\,|\Phi_l^-\rangle\,|\Phi_p^-\rangle\,. \tag{S48}
$$

We would like to remove the following component from the two-photon case since there is an extra phase δ that was introduced by the STIRAP interaction:

$$
(|1_l,0_p\rangle_A\,|1_l,0_p\rangle_B)\,|\Phi_l^+\rangle\,|\Phi_p^+\rangle \overset{4\times\mathrm{CZ}}{\to} (|1_l,0_p\rangle_A\,|1_l,0_p\rangle_B)\,|\Phi_l^+\rangle\,|\Phi_p^+\rangle\,. \tag{S49}
$$

Therefore if we measure the auxiliary $|\Phi^\pm\rangle$, we can distinguish between

1. When both the Bell pairs are in state $|\Phi^+\rangle$, this means no photon has arrived, or the system is in the "contaminated" two-photon state.
2. We have $|\Phi_l^-\rangle\,|\Phi_p^+\rangle$, which means exactly one photon has arrived.
3. We have $|\Phi_l^-\rangle\,|\Phi_p^-\rangle$, we have two photons in the system, where the phase component is $e^{i2\phi}$.

After the STIRAP interaction, the term $\sqrt{2}e^{i\phi}\,|1,1\rangle$ acquires an additional unwanted relative phase $e^{i\delta}$ due to coupling with the cavity, which we need to remove.

We can distinguish the zero-, single- and two-photon contributions by using parity checks on the memory qubits as well as the cavity photon state by using shared Bell states between Alice and Bob. The parity check on the cavity state can be achieved by introducing another auxiliary atom. We use the subscripts l to denote levels of an atomic system and p for photonic Fock states. We assume the Bell pairs $|\Phi^+\rangle$ are shared between Alice and Bob, where the subscript denotes which system they are paired with. For example,

$$
|1_l\rangle_A\,|0_l\rangle_B\,|\Phi_l^+\rangle \overset{2\times\mathrm{CZ}}{\to} |1_l\rangle_A\,|0_l\rangle_B\,|\Phi_l^-\rangle \tag{S50}
$$

denotes that 2 CZ gates are applied, where the control qubits are $|1_l\rangle_A\,|0_l\rangle_B$, and the target qubits are $|\Phi_l^+\rangle$.

For the zero photon cases:

$$
\begin{aligned}
&(|0_l,0_p\rangle_A\,|0_l,0_p\rangle_B)\,|\Phi_l^+\rangle\,|\Phi_p^+\rangle \overset{4\times\mathrm{CZ}}{\to}\\
&(|0_l,0_p\rangle_A)\,|1_l,1_p\rangle_B)\,|\Phi_l^+\rangle\,|\Phi_p^+\rangle\,.
\end{aligned}
\tag{S51}
$$

For the single photon case:

$$\begin{aligned}&(|1_l,0_p\rangle_A|0_l,0_p\rangle_B,|0_l,0_p\rangle_A|0_l,1_p\rangle_B)|\Phi_l^+\rangle|\Phi_p^+\rangle \overset{4\times\mathrm{CZ}}{\rightarrow}\\&(|1_l,0_p\rangle_A|0_l,0_p\rangle_B,|0_l,0_p\rangle_A|0_l,1_p\rangle_B)|\Phi_l^-\rangle|\Phi_p^+\rangle\,.\end{aligned}\tag{S52}$$

For the two photon cases:

$$\begin{aligned}&(|1_l,1_p\rangle_A|0_l,0_p\rangle_B,|0_l,0_p\rangle_A|1_l,1_p\rangle_B)|\Phi_l^+\rangle|\Phi_p^+\rangle \overset{4\times\mathrm{CZ}}{\rightarrow}\\&(|1_l,1_p\rangle_A|0_l,0_p\rangle_B,|0_l,0_p\rangle_A|1_l,1_p\rangle_B)|\Phi_l^-\rangle|\Phi_p^-\rangle\,.\end{aligned}\tag{S53}$$

We would like to remove the following component from the two-photon case, since there is an extra phase δ that was introduced by the STIRAP interaction:

$$\begin{aligned}&(|1_l,0_p\rangle_A|1_l,0_p\rangle_B)|\Phi_l^+\rangle|\Phi_p^+\rangle \overset{4\times\mathrm{CZ}}{\rightarrow}\\&(|1_l,0_p\rangle_A|1_l,0_p\rangle_B)|\Phi_l^+\rangle|\Phi_p^+\rangle\,.\end{aligned}\tag{S54}$$

Therefore if we measure the auxiliary $|\Phi^{\pm}\rangle$, we can distinguish between

1. When both the Bell pairs are in state $|\Phi^+\rangle$, this means no photon has arrived, or the system is in the"contaminated" two-photon state.
2. We have $|\Phi_l^-\rangle|\Phi_p^+\rangle$, which means exactly one photon has arrived.
3. We have $|\Phi_l^-\rangle|\Phi_p^-\rangle$, we have two photons in the system, where the phase component is $e^{i2\phi}$.